



1 **Warming accelerates the decomposition of root biomass in a** 2 **temperate forest only in topsoil but not in subsoil**

3 **Binyan Sun¹, Cyrill Zosso^{1,3}, Guido L. B. Wiesenberg¹,**
 4 **Elaine Pegoraro², Margaret S. Torn², and Michael W. I. Schmidt¹**

5
 6 ¹University of Zurich, Department of Geography, Zurich, Switzerland.

7 ²Climate and Ecosystem Sciences Division, Lawrence Berkeley National Laboratory,
 8 Berkeley, CA, USA.

9 ³Agroscope, Switzerland

10 *Correspondence to:* Binyan Sun, binyan.sun@geo.uzh.ch

11

12 **Abstract.**

13 Global warming could potentially increase the decomposition rate of soil organic matter
 14 (SOM), not only in the topsoil (< 20 cm) but also in the subsoil (> 20 cm). Despite its low
 15 carbon content, subsoil holds on average nearly as much SOM as topsoil across various
 16 ecosystems. However, significant uncertainties remain regarding the impact of warming on
 17 SOM decomposition in subsoil, particularly root-derived carbon, which serves as the primary
 18 organic input at these horizons. In the Blodgett Forest warming experiment (California, USA),
 19 we investigated whether warming accelerates the decomposition of root-litter at three depths
 20 (10-14, 45-49, and 85-89 cm) by using molecular markers and *in-situ* incubation of ¹³C-labelled
 21 root-litter at each depth. Our results reveal that the decomposition of added root-litter was only
 22 accelerated in the topsoil (10-14 cm) but not in the subsoil (45-49 and 85-89 cm) with warming.
 23 In subsoil, although the decomposition rate of root-litter derived carbon did not differ
 24 significantly between ambient and warmed plots, the underlying reasons for this similarity are
 25 distinct. With molecular marker analysis, we found higher microbial activity, indicated by
 26 higher concentration of certain fatty acid monomers that could be originally microbial-derived
 27 such as octadecanoic acid (C_{18:0} fatty acids), octadecenoic acid (C_{18:1} fatty acids), and
 28 hexadecanoic acid (C_{16:0} fatty acids) than those originally derived from roots in ambient
 29 subsoil. With warming, the higher concentration of long-chain (C number > 20) ω-hydroxy
 30 acids and diacids left after 3 years of root incubation suggested a lower turnover rate and this
 31 could be due to lower microbial abundance and lower soil moisture induced by warming. Our



1 study demonstrates that the impact of warming on the decomposition of root-litter in a
2 temperate forest is depth-dependent. The slower turnover rate of long-chain ω -hydroxy acids
3 and diacids shows that they are more persistent compared to bulk root mass and could be
4 preserved in subsoil for longer time as long as the environmental conditions are unfavorable
5 for decomposition with warming.

6

7 **Keywords**

8 Soil warming, decomposition, subsoil, hydrolysable lipids, fine roots, priming

9

10 **Highlights**

11 Warming accelerates the decomposition of root-litter in the topsoil but not subsoil

12 Hydrolysable lipids are not resistant to warming in topsoil and could be preserved in subsoil
13 for with warming

14 No priming effects on the pre-existing bulk soil carbon and hydrolysable lipids after 3 years



15 **1. Introduction**

16 Global air temperatures are projected to increase between 2.6 °C and 4.8 °C by 2100 under
 17 Representative Concentration Pathway 8.5, according to the Intergovernmental Panel on
 18 Climate Change (IPCC, 2013). In synchrony with air temperature, soil temperature is also
 19 expected to increase, not only in topsoil (< 20 cm) but also in subsoil (> 20 cm) (Soong et al.,
 20 2020). Global soils hold the largest actively cycling terrestrial carbon pool and store between
 21 2000 Pg and 3000 Pg of carbon in the top 3 m, with over 50% located in subsoil (Scharlemann
 22 et al., 2014). Previous studies demonstrated that warming could accelerate the decomposition
 23 of soil organic matter (SOM) in topsoil (Scharlemann et al., 2014), as well as in subsoil (Hicks
 24 Pries et al., 2017; Soong et al., 2021), potentially causing loss of CO₂ to the atmosphere.
 25 Moreover, enhanced temperature accelerated the decomposition of complex polymeric organic
 26 matter (OM) (Ofiti et al., 2023; Zosso et al., 2023), which had been regarded as comparatively
 27 recalcitrant to microbial decomposition.

28 Often, manipulative field warming experiments have focused on topsoil (Chen et al.,
 29 2022; van Gestel et al., 2018; Melillo et al., 2017; Verbrigghe et al., 2022), both in terms of the
 30 soil depths warmed by the manipulation and focus of the investigation. Therefore, it remains
 31 unclear from these experiments if the deeper soil horizons respond in similar ways to
 32 environmental changes as topsoil, since biotic and abiotic properties differ. Subsoil SOM has
 33 been assumed to be relatively insensitive to warming, because larger proportions of this deep
 34 SOM are more spatially inaccessible to microorganisms due to their associations to mineral
 35 surfaces compared to surface soil (Lützow et al., 2006). Furthermore, the microbial abundance
 36 varies throughout the soil profile (Rumpel et al., 2012; Zosso et al., 2021). Microbial biomass
 37 is substantially higher in topsoil than in subsoil (Naylor et al., 2022), by as much as two orders
 38 of magnitude (Fierer et al., 2003), leading to significantly slower turnover of carbon in the
 39 subsoil (Spohn et al., 2016). Also, microbial community structure changes with depth. Across
 40 different ecosystems, there is generally a proportional increase of Gram-positive to Gram-
 41 negative bacteria with depth (Eilers et al., 2012; Xu et al., 2021; Zosso et al., 2021) due to
 42 decreased carbon availability and quality (Fanin et al., 2019; Naylor et al., 2022). With
 43 warming, the difference in microbial abundance and composition between topsoil and subsoil
 44 could become more pronounced (Fontaine et al., 2007; Zosso et al., 2021), leaving large
 45 uncertainties of the impact on SOM decomposition at different depths.



One of the most important biotic factors could change the SOM dynamics in the subsoil is root mass. Compared to topsoil, root mass is one of the major carbon sources in the subsoil (Button et al., 2022; Rumpel and Kögel-Knabner, 2011), especially in seasonally dried temperate evergreen forest, where root depth could be deep (Schenk and Jackson, 2005). Moreover, roots impact on SOM dynamics in subsoil in two way: They are more likely to form stable SOM (Jackson et al., 2017; Rasse et al., 2005; Sokol and Bradford, 2019) to aboveground plant biomass, and they also could stimulate the microbial mineralisation of preserved SOM in subsoil, leading to loss of old and pre-existing SOM (Dijkstra et al., 2021; Fontaine et al., 2007). However, the scientific debate continues, how root and SOM interaction will alter under global warming, specifically in the subsoil. Previous studies showed a variety of responses root biomass in the surface soil to warming, with either more fine root biomass (Kwatcho Kengdo et al., 2022; Malhotra et al., 2020; Wang et al., 2021), less root biomass (Arndal et al., 2018; Ofiti et al., 2021), or no change in root biomass (Wang et al., 2017). In subsoil, it is assumed that roots will forage in deeper soil horizons under water stress induced by warming (Wang et al., 2021, 2017), but the opposite was observed in a warming experiment in a temperate forest with a substantial loss of fine roots (< 2 mm) and coarse roots (2-5 mm) (Ofiti et al., 2021) across the soil profile after 4 years of warming. Additionally, it was also observed that warming (Parts et al., 2019; Yaffar et al., 2021) or higher temperature induced drought (Meier and Leuschner, 2008) increased mortality of fine root biomass. Since this root-litter could serve as new substrates for carbon-limited subsoil horizons and fuel decomposition of pre-existing carbon, it is important to understand how microorganisms will respond to this new input at different depths under warming conditions.

Besides, previous studies exhibited evidence of carbon loss with warming (Soong et al., 2021), mainly by rapid decomposition of decadal-aged carbon (Hicks Pries et al., 2017), but they did not provide information of the transformation of new carbon input and soil C formation at molecular level. Molecular proxies or markers such as plant-derived hydrolysable lipids suberin, which mainly derive from woody tissues such as roots (Kolattukudy, 1980), could be used as quantitative and qualitative methods to follow alterations of root-derived carbon during decomposition and determine their turnover rate when in combination with compound-specific ^{13}C isotopic analysis (Feng et al., 2010). It is also very important to know whether these molecular proxies could be preserved under warming since harnessing roots, especially to increase their hydrolysable lipids content, is regarded as one of the solutions to mitigate climate change (Eckardt et al., 2023).



79 Many previous studies on the mechanisms of the interaction between root-derived
 80 carbon and soil (decoupling carbon from mineral protection or formation of soil C) were
 81 conducted as laboratory incubation experiments (Keiluweit et al., 2015; Sokol and Bradford,
 82 2019). Such techniques with high replicability and controlled conditions contribute to
 83 understanding certain soil carbon transformation or stabilization processes. However,
 84 laboratory incubations are usually far from natural conditions and lack many of the biotic or
 85 abiotic interactions that occur in soil *in-situ*.

86 Therefore, in our study, we used a multi-year, whole-soil-profile warming experiment,
 87 located at the University of California Blodgett Experimental Forest, to study the effect of
 88 warming on the decomposition of root-litter at different soil depths (10-14 cm, 45-49 cm, and
 89 85-89 cm). We incubated ^{13}C -labelled roots *in-situ* for three years, to understand how the
 90 decomposition of root-derived carbon varies with depth and warming. Specifically, we
 91 determined the quantity of different monomers in hydrolysable lipids, released from polymeric
 92 SOM. For each monomer we investigated stable carbon isotope values ($\delta^{13}\text{C}$) by compound-
 93 specific ^{13}C isotope analysis to understand how quickly root-derived carbon and hydrolysable
 94 lipids degrade at different soil depths with warming. We hypothesized that first: warming
 95 would accelerate the decomposition of root biomass and root-derived hydrolysable lipids
 96 across the whole soil profile regardless of soil depths. Second, we expect a relative
 97 accumulation of hydrolysable lipids in the root-derived carbon because they are commonly
 98 regarded as chemically persistent compounds (Lorenz et al., 2007).

99 **2. Material and methods**

100 **2.1 Study site**

101 The whole-soil warming experiment at University of California Blodgett Experimental
 102 Forest is located on the foothills of the Sierra Nevada near Georgetown, CA (120°39'40"W;
 103 38°54'43"N) at 1370 m above sea level (Hicks Pries et al., 2018). The site has a Mediterranean
 104 climate with a mean annual air temperature of 12.5 °C and a mean annual precipitation of 1774
 105 mm (Bird and Torn, 2006). The experiment is situated in a thinned 80-year-old mixed
 106 coniferous temperate forest, dominated by ponderosa pine (*Pinus ponderosa*), sugar pine
 107 (*Pinus lambertiana*), incense cedar (*Calocedrus decurrens*), white fir (*Abies concolor*), and
 108 douglas fir (*Pseudotsuga menziesii*) (Hicks Pries et al., 2017). The soils are Holland series and
 109 classified as fine-loamy, mixed superactive, mesic ultic Alfisol of granitic origin (mean pH
 110 5.5).



111 Briefly, the whole-soil warming experiment consists of 6 plots in total arranged in three
 112 replicated blocks, each having a pair of warmed and controlled circular plots 3 m in diameter.
 113 Soils in warmed plots were 4 °C above ambient temperature to 1 m depth while the natural
 114 temperature gradient with depth was maintained following the design described previously
 115 (Hicks Pries et al., 2017). To maintain warming down to 1 m depth, twenty-two 2.4-m-long
 116 resistance heating cables (BriskHeat, Ohio, USA) were vertically installed in metal conduits at
 117 a radius of 1.75 m, surrounding each plot. Two concentric rings of surface heater cable were
 118 installed at 1 and 2 m in diameter, 5 cm below the soil surface, to compensate for surface heat
 119 loss. The setup of the control plots is identical to the warmed plots but without heating cables
 120 placed inside the metal conduits (Hicks Pries et al., 2017).

121 2.2 ¹³C-labelled root-litter experiment and sampling

122 Common wild oat (*Avena fatua*) is an annual grass, and its roots were used as a model
 123 substrate in this experiment (Hicks Pries et al., 2018). *Avena fatua* seedlings were grown for
 124 12 weeks in a greenhouse within an airtight chamber at the University of California, Berkeley.
 125 Every 4 days the source of CO₂ was switched between ambient CO₂ and 10 atom% ¹³CO₂
 126 (Cambridge Isotope Laboratories, Inc., Massachusetts, USA) (Castanha et al., 2018; Hicks
 127 Pries et al., 2018). After this labeling phase, roots were excavated, dried and cut in 1-2 cm
 128 pieces (< 2 mm diameter).

129 A total of six soil cores were prepared in each plot by using a perforated custom coring
 130 system made of polycarbonate and aluminum tubes (5.04 cm outer diameter and 4.41 cm inner
 131 diameter). Each core consisted of four polycarbonate sections (10 cm, 35 cm, 40 cm, and 10
 132 cm in length, respectively) that were threaded on each end (male threads) and connected with
 133 female-to-female threaded polycarbonate connectors. The aluminum tube was screwed onto
 134 each section of one core sequentially so that the polycarbonate sections could be hammered in
 135 the soil for coring. The top 4 cm of soil in each section was marked and scooped into aluminum
 136 tins. A pre-weighed, aliquot of 0.14 g. *Avena fatua* fine roots (0.463 g C g root⁻¹, 5.6% atom
 137 ¹³C) (Castanha et al., 2018; Hicks Pries et al., 2018) were added to three soil depths (10-14 cm,
 138 45-49 cm, and 85-89 cm) of four out of the six cores which were referred to as root treatment.
 139 The labelled roots were added and mixed in. The other two cores without labelled roots but
 140 with the same disturbance were used as disturbance controls (DC). For disturbance control,
 141 the soil was mixed without root addition. After adding roots to each target depth, the core
 142 sections were connected by the female-to-female connectors and the resulting 95 cm long core



143 was placed back in the hole from which it originated. In July 2019, i.e., after three years of *in-*
 144 *situ* field incubation, two root treatment and one disturbance control cores were retrieved from
 145 each plot. The retrieved cores were wrapped in aluminum foil and transported to Lawrence
 146 Berkeley National Laboratory and stored in a -20°C freezer before further processing.

147 **2.3 Soil preparation and characterization**

148 In the results and discussion for this paper, the topsoil denotes the soil depth at surface
 149 (10-14 cm) and the subsoil describes the soil depths at 45-49 cm (mid-depth) and 85-89 cm
 150 (deep soil). In the laboratory, we opened the polycarbonate cores to retrieve the 4 cm section
 151 where labelled roots were added (same for disturbance control). We also sampled the 4 cm
 152 section above and below the target depths. The soil samples were sieved <2 mm. Roots were
 153 picked off the top of the sieve by tweezers. Bulk soil <2 mm was freeze-dried and re-weighed.
 154 A subsample of bulk soil samples was ground by a ball mill (MM400, Retsch, Haan, Germany)
 155 and analyzed for carbon and nitrogen concentrations, as well as stable carbon isotope
 156 composition ($\delta^{13}\text{C}$) using an elemental analyzer-isotope ratio mass spectrometer (EA-IRMS;
 157 Flash 2000-HT Plus, linked by Conflo IV to Delta V Plus isotope ratio mass spectrometer,
 158 Thermo Fisher Scientific, Bremen, Germany). The results are reported in the δ notation:

$$159 \quad \delta^{13}\text{C} = \left(\frac{R_{\text{sample}}}{R_{\text{standard}}} - 1 \right) \times 1000 \quad (1)$$

160 Where R_{sample} and R_{standard} are the $^{13}\text{C}/^{12}\text{C}$ ratios of the sample and the international
 161 standard, Vienna Pee Dee Belemnite (VPDB, 0.01118), respectively. At least two analytical
 162 replicates were measured for all samples. Calibration was carried out using IAEA-certified
 163 primary standards (e.g., N600 caffeine) and caffeine (Merck) as secondary standard.

164 **2.4 Analysis of hydrolysable lipids**

165 All soil samples (< 2 mm) were pre-extracted by Soxhlet following an established
 166 protocol (Wiesenberg and Gocke, 2017) to remove solvent-extractable lipids with
 167 dichloromethane (DCM): methanol (93:7; v/v) for 48 hours. The extraction residues were dried
 168 until constant weight.

169 The extraction residues were homogenized with a ball mill (MM400, Retsch, Haan,
 170 Germany) and then hydrolyzed according to (Zosso et al., 2023)(2023). Therefore, an aliquot
 171 of each residue equivalent to > 20 mg carbon was weighed in a 250 mL round bottom flask.
 172 The sample was mixed with the extraction solution methanol: deionized water (9:1; v/v) with
 173 6% potassium hydroxide (KOH) and then saponified for 20 hours at around $85-88^{\circ}\text{C}$ in a water



174 bath under reflux. Subsequently, the solution was filtered and transferred to a separation funnel
 175 for phase separation. The solution was acidified to pH 2.0 using 6 M hydrochloric acid (HCl)
 176 and then extracted with DCM. The collected fractions were volume-reduced and remaining
 177 water was removed by water-free sodium sulfate (Na₂SO₄).

178 For quantification of hydrolysable lipids, deuterated eicosanoic acid (D₃₉C₂₀;
 179 Cambridge Isotope Laboratories, Inc.) was added to the samples as an internal standard. The
 180 samples were silylated at 80 °C for 1 hour with bis(trimethylsilyl)acetamide (BSA)
 181 (Wiesenberg and Gocke, 2017). Individual compounds were quantified on an Agilent 7890B
 182 gas chromatograph (GC) equipped with a multi-mode inlet and a flame ionization detector
 183 (FID). Compound identification was performed on an Agilent 6890N GC equipped with
 184 split/splitless inlet and coupled to an Agilent 5973 mass selective detector (MS). Compounds
 185 were identified by comparison of mass spectra with those of external standards and from the
 186 NIST and Wiley mass spectra library. Both instruments were equipped with DB-5MS columns
 187 (50 m × 0.2 mm × 0.33 μm) and 1.5 m de-activated pre-columns, with helium as the carrier gas
 188 (1 ml min⁻¹). Silylated fractions were injected in splitless mode at an initial GC oven
 189 temperature of 50 °C that was kept isothermal for 4 min, then increased to 150 °C at a rate of
 190 4 °C min⁻¹. Thereafter, the temperature ramped up to 320 °C at a rate of 3 °C min⁻¹ and held for
 191 40 min. The GC-MS was operated in electron ionization mode at 70 eV and scanned from m/z
 192 60-650. The analysis of the data was processed with Agilent Chemstation software. The
 193 concentration of each compound was finally normalized to the organic carbon concentration of
 194 the respective sample (stated as μg g⁻¹ OC). The weight of samples weighed in for
 195 hydrolyzation is always corrected by accounting for the mass loss due to free lipid extraction:

$$196 \quad M_{corrected} = \frac{M_{weighed}}{(1 - p_{free\ lipids})} \quad (2)$$

197 Where $M_{corrected}$ is the corrected weight of soil samples, $M_{weighed}$ is the weight of soil
 198 samples weighed in for hydrolyzation, and $p_{free\ lipids}$ is the proportion of free extractable lipids
 199 to the mass of soil samples weighed in for Soxhlet extraction.

200 In this paper, mid-length and long-chain monomers are the compounds with a carbon
 201 chain length n between 14 and 20 ($14 \leq n < 20$) and length ≥ 20 , respectively. For each
 202 compound class, n -carboxylic acids are the synonymously used for n -fatty acids, ω -
 203 hydroxy acids are short for ω -hydroxy carboxylic acids, diacids stand for α , ω -alkanedioic
 204 acids, alcohols are abbreviated for n -alcohols, and mid-chain acids stand for mid-chain
 205 hydroxylated fatty acids, referring to fatty acids with functional groups or structural



modifications located in the middle of their carbon chain, typically at the C-9 and C-10 carbon positions, such as ω -dihydroxyhexadecanoic acid ($x = 9$ or 10) (Graça, 2015).

Different monomers can be used as markers for leaf and needle (cutin) or woody and root (suberin) biomass. However, there are no universal markers across a variety of studies since the relative proportions of cutin and suberin markers could vary among plant taxa, plant functional type or plant organ (Jansen and Wiesenberger, 2017; Mueller et al., 2012). Here, we selected ω -hydroxy alkanic acids and diacids as suberin markers since these monomers exist in substantial amount in the roots of the dominating plant species around the experiment plots and are 10 times higher in concentration compared to the same monomers in leaves or needles in the same species (Supplementary Fig. S2). Cutin markers could not be distinguished since all the mid-chain acids which were traditionally considered as cutin markers were present in considerable amounts both in leaves/needles and roots in the analyzed plants (Supplementary Table S1).

To the best of our knowledge, there are no studies reporting the composition of mid-chain fatty acids, ω -hydroxy or diacids from microorganisms in soil, although it was reported that microorganisms can synthesize the compound classes mentioned above (Huf et al., 2011; Kim and Park, 2019). These compound classes, however, are more region-specific and differ from those in plants and animals (Kim and Oh, 2013) and usually have a carbon chain-length < 20 (Zhang et al., 2024). Therefore, we hypothesize that all the compounds with a carbon chain length ≥ 20 and mid-chain fatty acids are exclusively plant-derived.

2.5 Compound-specific isotope analysis

To determine the $\delta^{13}\text{C}$ of individual compounds, a Trace GC Ultra, coupled via GC Isolink II and Conflo IV to Delta V Plus isotope mass spectrometer (Thermo Fisher Scientific) was used to perform compound-specific $\delta^{13}\text{C}$ analysis of individual hydrolysable lipids. The settings of the instrument and temperature program used here was the same as mentioned above. Reproducibility and stability ($< 0.6\%$) of $\delta^{13}\text{C}$ values were checked with pulses of CO_2 reference gas and n -alkane standard mixture (C_{20-30} ; Sigma Aldrich) of known isotope composition. The $\delta^{13}\text{C}$ values were presented in per mil (‰) relative to the Vienna-Pee Dee Belemnite (V-PDB) reference standard. Every sample was measured with three analytical replicates and the difference between measurements typically did not exceed 1.0 ‰ for natural abundance samples and 10% of the measured isotope value for ^{13}C labelled samples.



2.6 Calculations

The isotope composition of individual hydrolysable lipids was corrected for the value of the $\delta^{13}\text{C}$ value of each trimethylsilyl group that was added during silylation as:

$$\delta_{UD} = \frac{(n+3 \times a) \times \delta_D - 3 \times a \times \delta_M}{n} \quad (3)$$

Where n is the number of C atoms in the underivatized hydrolysable lipids and δ_{UD} and δ_D are isotope ratios of the underivatized and the derivatized hydrolysable lipids, respectively, a is the number of functional groups in individual compounds that were derivatized by BSA. δ_M is the C isotope ratio of the added trimethylsilyl group (-44.3‰). δ_M was determined by repeated measurement ($n = 8$, with 3 analytical replicates of each) of derivatized standard FAs (C_{10} and C_{12} FAs with known $\delta^{13}\text{C}$ isotope composition).

The ^{13}C -excess, which can be expressed as percent atom excess, presents the enrichment of ^{13}C in individual hydrolysable lipids. The value is defined as the ratio of the relative abundance of the heavier stable isotope in a labelled sample to the natural isotope abundance in the identical unlabelled sample (Epron et al., 2012). It was calculated as followings (Speckert et al., 2023):

$$^{13}\text{C} - \text{excess}[\%] = \left(\frac{100}{^{13}\text{C}/^{12}\text{C}_{\text{distcontrol}}} \times ^{13}\text{C}/^{12}\text{C}_{\text{labelled}} \right) - 100 \quad (4)$$

Where $^{13}\text{C}/^{12}\text{C}_{\text{distcontrol}}$ is the atomic ratio of the stable isotopes in the compartments (bulk soil carbon, and individual monomers of hydrolysable lipids) of the disturbance control plots as natural abundance values, and $^{13}\text{C}/^{12}\text{C}_{\text{labelled}}$ is the atomic ratio in the corresponding compartments in the plots with added labelled root litter.

As individual isotope values can vary a lot in between different homologues for each compound-class specifically in isotope labeling experiments, a more meaningful measure was chosen to express the $\delta^{13}\text{C}$ values of the respective compound-classes that can be assigned to the same carbon source (Wiesenberg et al., 2008). The $\delta^{13}\text{C}$ values and ^{13}C -excess for the most abundant compound classes (n -alcohols, n -fatty acids, diacids, and ω -hydroxy acids) within the hydrolysable lipid fractions were calculated separately as weighted means of individual compounds within each compound class. This means within each compound class, weightings will be given to each monomer in this compound class (e.g., ω -hydroxy acids) based on the proportional contribution of individual monomer (e.g., C_{24} ω -hydroxy acids) to the total concentration of this compound class. Then for individual monomers, their weightings will be multiplied by their $\delta^{13}\text{C}$ values, and we sum up all the monomers identified to get the weighted mean $\delta^{13}\text{C}$ values for this compound class:



$$\mu_c = \sum_{i=a}^b (x_{ci} \times w_{ci}) \quad (5)$$

Where μ denotes the average value and subscript c represents different compound classes, x denotes the value of either $\delta^{13}\text{C}$ or ^{13}C -excess, a and b represent the lower and upper limits of the respective carbon number range, w_i indicates the relative abundance of the individual compounds within compound class c .

The amount of root carbon that was recovered in bulk soil was calculated by dividing the amount of ^{13}C -labelled root-derived carbon left in the soil by the amount of carbon added with the original labelled roots. The proportion of root-derived carbon (f_{root}) was estimated by using a simple mixing model (Hicks Pries et al., 2018):

$$^{13}\text{C atom}\%_{\text{sample}} = ^{13}\text{C atom}\%_{\text{DC}} \times f_{\text{soil}} + ^{13}\text{C atom}\%_{\text{root}} \times f_{\text{root}} \quad (6)$$

$$f_{\text{root}} + f_{\text{soil}} = 1 \quad (7)$$

$$\text{Recovery}_{\text{root}} = \frac{f_{\text{root}} \times M_{\text{soil}} \times C\%_{\text{soil}}}{0.14 \times 0.463} \quad (8)$$

Where $^{13}\text{C atom}\%_{\text{sample}}$ is the $^{13}\text{C atom}\%$ of soil samples where labelled root-litter was added; $^{13}\text{C atom}\%_{\text{DC}}$ is the $^{13}\text{C atom}\%$ of soil samples in the disturbance control plots; $^{13}\text{C atom}\%_{\text{root}}$ is the $^{13}\text{C atom}\%$ of initial ^{13}C labelled roots; f_{soil} and f_{root} are the proportion of carbon originally derived from native soil and labelled root-litter, respectively. M_{soil} is the mass of the soil sample and $C\%_{\text{soil}}$ is the carbon content of the corresponding soil sample. 0.14 is the mass of root-litter (g) added at individual soil depth and 0.463 is the carbon content of the added root-litter.

The decay rate, k , of initially added ^{13}C -labelled roots and root-derived hydrolysable lipids was calculated based on the following model (Olson, 1963):

$$-kt = \ln \frac{M_t}{M_0} \quad (9)$$

where M_0 is the mass of original roots or root-derived hydrolysable lipids, M_t denotes the mass of root-derived carbon or hydrolysable lipids at time t , and t is the duration of incubation which is three years in our study. The model assumes that M is a well-mixed carbon pool with first-order decay kinetics. The residence time is the reciprocal of k .

The priming effect of added ^{13}C labelled root-litter was calculated using the mass of carbon in DC cores at individual depths as background values. Then, based on the calculations shown in 2.6.4, the proportion of native SOM that is left in the labelled cores within the same plot after three years of incubation was calculated:

$$\text{Priming effect} = \frac{MSOM_I - MSOM_{DC}}{MSOM_{DC}} \quad (10)$$



Where $MSOM_I$ and $MSOM_{DC}$ denote native SOM left in labelled cores and SOM in DC cores. The priming effect for hydrolysable lipids was calculated with the same approach. One outlier is excluded in priming effect calculation at mid-depth in ambient plots.

2.7 Statistical analysis

All statistical analyses were performed in RStudio (Version 2024.09.1+394, Posit team, 2024) with R 4.4.2 (R: The R Project for Statistical Computing, 2025). Shapiro-Wilk test and Levene test were used to assess the normality and heteroscedasticity of the data. To analyse the impact of main effects and their interactions on response variables, linear mixed effects models, lmerTest package was used (Kuznetsova et al., 2017). Normality and homoscedasticity were visually checked via residual plots. We used Akaike's information criterion (AIC) to test whether different fixed effects structures could improve model fit. If we observed a heteroscedasticity of variance of residuals, we log-transformed the data.

Hydrolysable lipid concentrations in disturbance control plots were tested in response to warming treatment, depth, and their interactions. ^{13}C -excess of bulk soil was tested in response to carbon content, depth, warming, and their interactions. We examined the effect of warming, depth, and their interactions on root recovery. We investigated how different compound classes, depth, warming, and their interactions influence ^{13}C -excess and mass change of hydrolysable lipids. For the priming effect of bulk soil and hydrolysable lipids, we tested how they respond to warming, depth and their interactions. All analyses included paired plots nested in blocks as a random effect. We regarded results as significant when the p -values are lower than 0.05.



3. Results

3.1 Soils without litter incubation

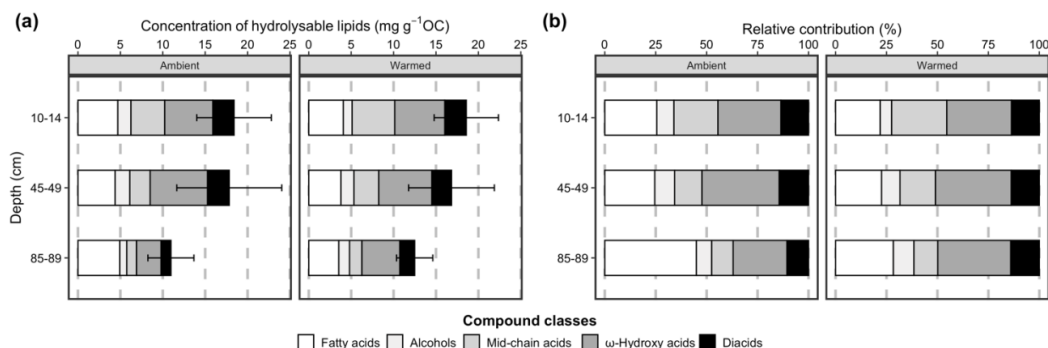


Figure 1: (a) Hydrolysable lipids normalized to soil organic carbon concentrations (mg g⁻¹OC) in disturbance control cores with ambient temperature (left) and warming (right) in 2019 after 3 years *in-situ* incubation (mean ± SE, n = 3); (b) Proportions of individual compound classes to total hydrolysable lipids identified in disturbance control cores (mean, n = 3). For clarity of the visual presentation SE error bars are shown cumulatively.

After three years of *in-situ* incubation, the average concentrations of hydrolysable lipids did not differ between ambient and warmed treatments, but they decreased with depth by the same amount under both treatments. These cores did not receive any ¹³C labeled root-litter, thus they tested how warming affected the abundance and composition of the pre-existing hydrolysable lipids at the experimental site. The concentrations of hydrolysable lipids were not different between ambient and warmed plots (LME; $p = 0.94$; $F = 0.006$) and depths (LME; $p = 0.17$; $F = 2.1$), with 18.4 ± 4.4 and 18.6 ± 3.8 mg g⁻¹ OC at topsoil and 17.8 ± 6.2 vs. 16.8 ± 5.1 mg g⁻¹OC at mid-depth in warmed and ambient plots, respectively. In the deep soil, the concentrations of hydrolysable lipids tended to be lower in the plots under ambient temperature (11.0 ± 2.7 mg g⁻¹OC) compared to warmed plots (12.5 ± 2.1 mg g⁻¹OC). We did not find interactions between warming and depths for concentrations of hydrolysable lipids (warming and depth, $p = 0.94$). Throughout results, the error bars represent standard errors.

To test how the hydrolysable lipid composition changed in between the three years of warming (i.e., between year 2016 and 2019) in the cores without litter incubation, we calculated the proportional contributions of individual compound classes to total hydrolysable lipids (Fig. 1b). The proportions of individual compounds in ambient temperature plots and warmed plots at topsoil and at mid-depth were similar. In contrast, in the deepest soil horizon, the proportions



of fatty acids were much higher under ambient temperature (45%) than in the warmed treatment (28%), leading to lower proportions of all the other compound classes in ambient plots.

With depth, the proportions of mid-chain hydroxy acids decreased regardless of temperature difference. In ambient and warmed plots, the proportion of mid-chain hydroxy acids consistently declined from topsoil (22% and 27% for ambient and warmed, respectively) to deep soil horizon (11% and 12%, respectively). In the warmed plots, the proportions of ω -hydroxy acids and diacids increased slightly from 45% in the topsoil to around 50% in mid-depth and deep soil. In the ambient plots, these lipids increased between topsoil (44%) to mid-depth soil (52%) but then decreased to deepest soil depth (37%).

3.2 Soils with root litter incubation

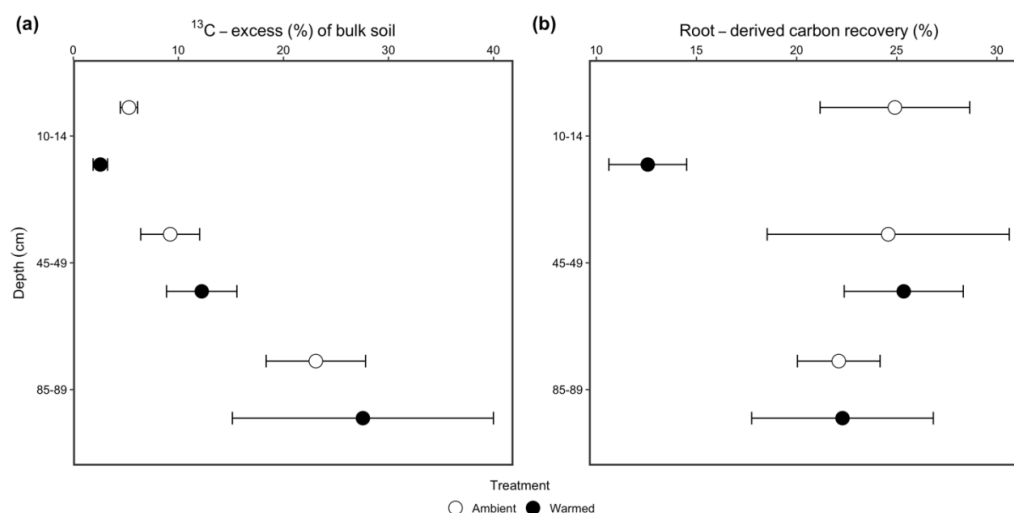


Figure 2: (a) The presence of carbon derived from the ^{13}C -labeled root in the bulk soil after three years of incubation, expressed as ^{13}C -excess of bulk soil carbon (Mean \pm SE, $n = 3$) at 10-14, 45-49, 85-89 cm depth in 2019 in ambient plots (white circles) and warmed plots (black circles). Error bars represent the standard error of the mean. (b) Proportions of the added root-derived carbon recovered after three years of incubation in bulk soil in ambient (white circles) and warmed plots (black circles). Mean \pm SE ($n = 3$).

We estimated the amount of added ^{13}C -labeled root-litter remaining after three years *in-situ* incubation as the ^{13}C -excess of bulk soil organic carbon.

Carbon concentration (LME; $p < 0.001$; $F = 78.54$), depth (LME; $p = 0.016$; $F = 13.83$) and their interaction (LME; $p = 0.005$; $F = 26.09$) had significant impact on ^{13}C -excess, whereas warming treatment (LME; $p = 0.42$; $F = 0.81$) did not. In topsoil, there were on average lower ^{13}C -excess values in warmed plots ($2.6 \pm 0.7\%$) than in ambient plots ($5.3 \pm 0.8\%$). In



subsoil, ^{13}C -excess was on average higher in warmed than ambient plots. At mid-depth, ^{13}C -excess was lower in ambient plots ($9.2 \pm 2.8\%$) than in warmed plots ($12.2 \pm 3.3\%$), but these differences were not significant. In deep soil, warmed-plot values had large variability but averaged higher ^{13}C -excess ($27.6 \pm 12.4\%$) compared to ambient plots ($23.1 \pm 4.7\%$). The standard error increased significantly with depth, especially in warmed plots in the deep soil.

The recovery of root-derived carbon was similar, regardless of depth (LME; $p = 0.151$; $F = 2.29$) or temperature treatment (LME; $p = 0.130$; $F = 2.72$), except for the warmed topsoil where the recovery was significantly lower in warmed ($13.6 \pm 1.9\%$) than the ambient-plot topsoil ($24.9 \pm 6.5\%$) (LME; $p = 0.011$). The interaction between warming and depth is close to the statistically significant threshold (LME; $p = 0.069$; $F = 3.53$), and this interaction is significant at mid-depth (LME; $p = 0.034$).

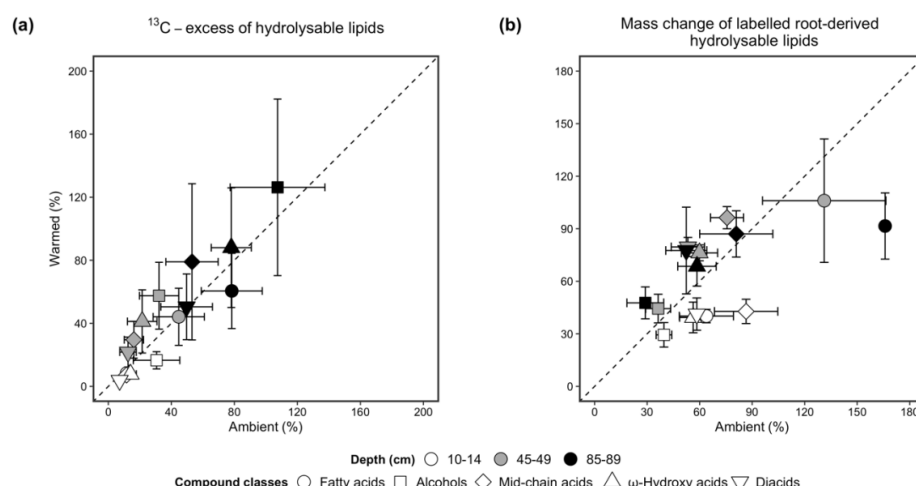


Figure 3: (a) Comparing the means of weighted ^{13}C -excess of each compound class from warmed plots (y-axis) and ambient plots at three depths (10-14 cm, 45-49 cm, 85-89 cm) with a 1:1 line $n = 3$; (b) Comparing of mean of mass change (%) of each compound class in hydrolysable lipids compared to those in the roots that were added to the soils for the *in-situ* incubation experiment. In both plots, the error bars denote the standard error of each compound class in ambient and warmed plots in the individual soil depths. Values smaller than 100% indicate a loss and those larger than 100% indicate a gain of this compound class. Values above the 1:1 line indicate higher values in warmed plots than in ambient plots and values below the 1:1 line indicate lower values in warmed plots than in ambient plots.

Similar to bulk soil organic carbon, the weighted ^{13}C -excess of each compound class increased with depth (LME; $p < 0.0001$; $F = 74.80$) (Fig. 3a). In topsoil, all compound classes had lower ^{13}C -excess in warmed plots than in ambient plots (LME; $p = 0.012$). Besides, the weighted ^{13}C -excess depends significantly on compound classes (LME; $p < 0.0001$; $F = 9.09$).



389 The decomposition of different compound classes at mid-depth and in deep soil were
 390 similar, except for fatty acids. The ^{13}C -excess of alcohols, mid-chain acids, ω -hydroxy acids,
 391 and diacids was on average higher in the warmed plots than in the ambient temperature plots,
 392 although the differences were not significant. The ^{13}C -excess of fatty acids was higher in
 393 warmed than ambient plots in subsoil, particularly in the deep soil. In the latter, warming led
 394 to, on average, much lower ^{13}C -excess of 60.5 ± 23.9 compared to ambient temperature (78.3
 395 ± 19.3), although statistically not significant (LME; $p = 0.219$). Similar to ^{13}C -excess of the
 396 bulk soil, the standard error was in general also larger in warmed than in ambient plots.

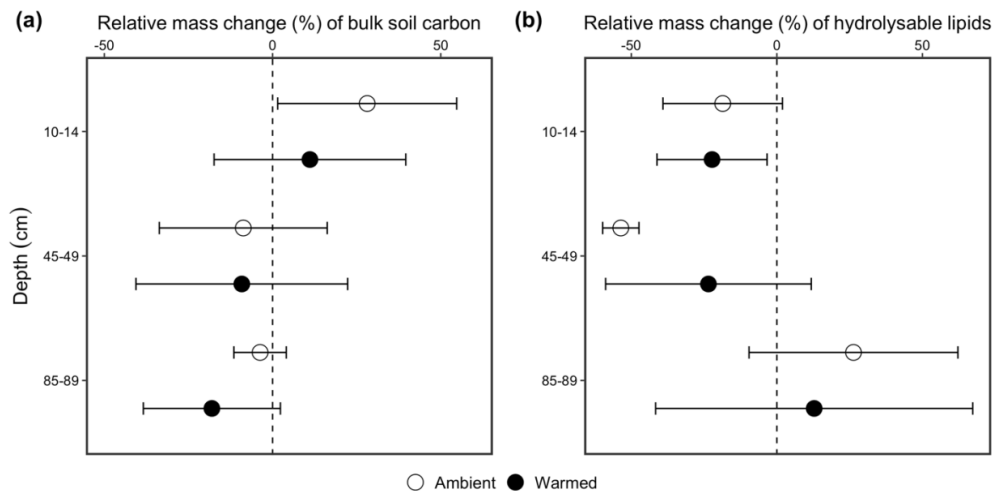
397 The differences of the absolute amounts of each compound class compared to added
 398 root-litter allowed us to quantify the loss or accumulation of each compound class after three
 399 years of incubation (Fig. 3b).

400 On the molecular level, as in bulk soil, warming did not have a significant impact on
 401 the decomposition of hydrolysable lipids (LME; $p = 0.518$; $F = 0.42$) across the whole soil
 402 profile but in the topsoil, decomposition was faster of all the compound classes compared with
 403 deeper soil depth (LME; $p = 0.001$). After three years of incubation the warmed topsoil had
 404 less hydrolysable lipids that derived from added labelled roots remaining compared to ambient
 405 temperature, indicated by higher loss of all the compound classes at this depth (Fig. 3b). After
 406 three years of incubation, the warmed topsoil had less than half of the initial compound classes
 407 left that was originally from the added as ^{13}C -labelled root-litter, i.e. $40.1 \pm 6.6\%$ of fatty acids,
 408 $29.4 \pm 12.1\%$ of alcohols, $42.8 \pm 12.0\%$ of mid-chain acids, $39.4 \pm 15.2\%$ of ω -hydroxy acids,
 409 and $41.3 \pm 16.0\%$ of diacids. More of each compound class was remaining in ambient plots,
 410 i.e., $63.8 \pm 26.8\%$ of fatty acids, $39.6 \pm 7.7\%$ of alcohols, $86.5 \pm 31.3\%$ of mid-chain acids,
 411 $56.3 \pm 13.4\%$ of ω -hydroxy acids, and $58.4 \pm 4.2\%$ of diacids, respectively (Fig. 3b).

412 Similar to the pattern observed for the ^{13}C -excess of individual hydrolysable lipids (Fig.
 413 3a), fatty acids and other compound classes showed an opposite trend (LME; $p < 0.001$; $F =$
 414 14.99) in subsoil when compared to topsoil (Fig. 3b). At both mid-depth and deep soil with
 415 ambient temperature, there was a trend to a higher loss of each compound class due to microbial
 416 decomposition compared to warmed plots except for fatty acids (Fig. 3b). On the contrary, fatty
 417 acids seemed to accumulate more under ambient temperature in subsoil ($131.2 \pm 32.3\%$ at 45-
 418 49 cm and $165.9 \pm 1.8\%$ at 85-89 cm), than with warming ($106.0 \pm 35.2\%$ for 45-49 cm and
 419 $91.6 \pm 18.9\%$ for 85-89 cm) (Fig. 3b). Specifically, the values above 100% indicate an
 420 enrichment of ^{13}C compared with the added root biomass over time, which was a surprising
 421 finding.



422 **3.3 Priming effect**



423 Figure 4: Relative mass difference of: (a) pre-existing bulk soil organic matter and (b) hydrolysable lipids
424 between cores with and without addition of ^{13}C -labeled root-litter (labelled – DC cores). Negative values indicate
425 the accelerated decomposition of pre-existing soil organic carbon (positive priming effect). Positive values
426 indicate inhibition (negative priming) of decomposition. Mean \pm SE (n = 3).

427 Overall, there are no significant impacts of warming (LME; $p = 0.558$; $F = 0.37$) or
428 depth (LME; $p = 0.422$; $F = 0.95$) on the priming effect. In the bulk topsoil, addition of ^{13}C
429 labeled root-litter reduced the decomposition (negative priming) of pre-existing SOM in topsoil
430 independent of temperature treatments (Fig. 4a). There was $28.1 \pm 26.6\%$ and $11.1 \pm 28.5\%$
431 more pre-existing SOM in the labelled cores than in the DC with ambient temperature and
432 warming, respectively. In contrast to topsoil, the subsoil showed the opposite trend. At both
433 mid-depth and deep soil, we observed a loss of pre-existing SOM upon addition of root litter,
434 regardless of temperature.

435 For the hydrolysable lipids, similar to bulk soil, we did not find significant impacts of
436 either warming (LME; $p = 0.987$; $F = 0.0002$) or depth (LME; $p = 0.310$; $F = 1.34$) on the
437 priming effect. We observed a reverse trend at topsoil and deep soil compared to bulk soil
438 (Fig. 4b). In the topsoil, addition of root-litter led to the loss of pre-existing hydrolysable lipids
439 in ambient ($-18.6 \pm 20.5\%$) and warmed ($-22.3 \pm 18.9\%$) plots. Thus, positive priming occurred.
440 This positive priming happened also at mid-depth, where added labelled root-litter stimulated
441 the loss of pre-existing hydrolysable lipids in both ambient ($-53.6 \pm 5.1\%$) and warmed
442 ($-23.5 \pm 35.3\%$) plots. However, in deep soil, there was negative priming, regardless of temperature



443 treatment (ambient, $26.3 \pm 35.9\%$; warmed, $12.8 \pm 54.5\%$). But the heterogeneity also increased
 444 with depth as indicated by generally increasing standard errors.

445 **4. Discussion**

446 After three years of *in-situ* $+4^{\circ}\text{C}$ warming, we observed different trends for
 447 decomposition of added ^{13}C -labelled root-litter between top- and subsoil both at bulk soil and
 448 molecular level. Soil warming altered several factors that could govern the decomposition rate
 449 of added root-litter such as microbial abundance, community structure (Zosso et al., 2021) and
 450 soil water content (Pegoraro et al., submitted), and these changes could potentially further
 451 affect microbial activity through reduced accessibility of substrates to exoenzymes or
 452 microorganisms under warming conditions (Salomé et al., 2010). The warming effects further
 453 interact with different abiotic and biotic conditions between top- and subsoil, leading to distinct
 454 depth-dependent decomposition of added root-litter at different soil horizons.

455 **4.1 Warming accelerated the decomposition of root-litter in topsoil, but not in subsoil**

456 The same amount of root-litter was added to all depths, and thus initial ^{13}C -excess
 457 increased with depth, as soil organic carbon concentrations decreased. After three years of field
 458 incubation, this general trend was still preserved.

459 Root biomass decomposition responded differently to experimental warming in topsoil
 460 and subsoil. On average, we found lower ^{13}C -excess of bulk SOM in topsoil under warming
 461 (Fig. 3a) compared to ambient conditions, indicating that warming accelerated the
 462 decomposition of the ^{13}C -labelled root-litter in topsoil ($p = 0.01$). This finding confirms
 463 previous observations from the same site, where warming accelerated decomposition of plant-
 464 derived inputs and increased soil respiration (Ofiti et al., 2021; Soong et al., 2021). There could
 465 be several reasons: First, at the same site, after 4 years of warming, there was an increase of
 466 carbon stock and free particulate organic matter in the topsoil (Soong et al., 2021), meaning
 467 there is sufficient easily decomposable substrate for microbial growth. This argues for co-
 468 metabolic decomposition of the added root litter, despite its lower decomposability than bulk
 469 carbon (Poirier et al., 2018). Therefore, microbial abundance was not significantly reduced by
 470 warming in topsoil (Zosso et al., 2021; Pegoraro et al., submitted). Second, warming enhanced
 471 microbial activity (Walker et al., 2018), potentially by activating a greater number of bacterial
 472 taxa (Metze et al., 2024). Third, because of more active bacteria and reorganization of microbial
 473 community towards more actinobacteria which could degrade more complex carbon sources



(DeAngelis et al., 2015; Goodfellow and Williams, 1983), a wider range of complex C and N sources could be utilized by microbes (Dove et al., 2021) compared to ambient plots.

In the subsoil, we did not observe significant effects of depth (45-49 cm, $p = 0.81$; 85-89 cm, $p = 0.64$) on the decomposition of added root-litter. However, the interaction between warming and depth in subsoil is significantly more pronounced (warming x 45-49 cm, $p = 0.03$) or close to the threshold of statistical significance level (warming x 85-89 cm, $p = 0.06$). This means that warming has depth-specific effects on the decomposition of added root-litter, highlighting the variability of subsoil compared to topsoil or even within subsoil between different depths. One reason could be the soil moisture. In ambient plots, the average annual soil volumetric water content increased with depth from 19.4 % (CI: 16.4, 22.2) to 90 cm by 10.5 % (CI: 8.1, 12.9) in ambient plots (Pegoraro, et al., submitted). Warming decreased soil moisture significantly at surface soil and at 90 cm, whereas soil moisture levels converged between warmed and ambient plots at 50 cm (Pegoraro, et al., submitted). Higher soil moisture increases the mobility of SOM, microorganisms, and exo-enzymes, which will allow the translocation of fresh C and decomposers (Védère et al., 2022) and then increases the connectivity among them (Védère et al., 2020), potentially resulting in higher decomposition rate. Another reason could be changes in microbial abundance and microbial community induced by warming. Warming decreases microbial abundance, especially in deep soil, and shifts microbial community towards relatively more actinobacteria and Gram+ bacteria which can utilize more complex carbon sources and adapt to environmental stress such as warming (Zosso et al., 2021). If bacteria could access the substrate, they could be more active under warming conditions. The cumulative effects of the two factors could compensate for each other and lead to on average no difference of root recovery in subsoil between warmed and ambient plots. However, they can only partially explain the results, since other factors such as oxygen, SOM protected by mineral-associations, pH could also have impacts on the variability between different depths.

Overall, our results reveal more complex responses of root-litter decomposition in subsoil under warming conditions in comparison to more straightforward acceleration of root-litter decomposition in topsoil.

4.2 Hydrolysable lipids are more resistant to decomposition than bulk roots

Root-derived hydrolysable lipids, especially those root-derived markers such as ω -hydroxy acids and diacids, degraded slower than root bulk carbon, indicated by higher



506 proportions of hydrolysable lipids remaining in the soil than the bulk root recovery (Fig. 2b,
 507 Fig. 3b). However, despite their higher resistance to decomposition compared to other root
 508 components, they resisted less to decomposition in warmed topsoil. One possible reason could
 509 be that the microbial population was well-adapted to the higher temperature and was able to
 510 harness complex biomass sources via hydrolytic processes (Dove et al., 2021; Zosso et al.,
 511 2021). The reported increased relative abundance of actinobacteria with warming in this
 512 experiment (Pegoraro et al., submitted) was similar to some other findings (DeAngelis et al.,
 513 2015; Pold et al., 2016). Since actinobacteria are assumed to decompose complex carbon
 514 sources (Bhatti et al., 2017) and are a main group of soil microorganisms producing hydrolytic
 515 enzymes (Mohan and El-Halwagi, 2007), the relative increase of actinobacteria could have
 516 capitalized on the warmed conditions and have accelerated the decomposition of added root
 517 litter. However, this acceleration of hydrolysable lipids could be only traced in topsoil with
 518 warming. Although the amount of the roots added to subsoil is proportionally more substantial
 519 compared to that added to topsoil, especially for deep soil (proportionally contribution to pre-
 520 existing carbon ranging from 10% to 39%), this short-term new substrate did not result in long-
 521 term faster mineralization of root-litter with warming at depth. There may be an initial quick
 522 response of microbial mineralization to added root-litter at the beginning of the experiment,
 523 but this faster decomposition could be slowed down over time as the added litter becomes more
 524 fragmented and depleted at depth. This pattern of decomposition with depth, which evolves
 525 over time, has also been observed in another root-litter decomposition experiment (Hicks Pries
 526 et al., 2018). However, since we don't have time resolved observations for our experiment, this
 527 argument cannot be confirmed. With continuing warming, microbial capacity to utilize root-
 528 litter could further deteriorate by lower microbial abundance, unfavorable environmental
 529 conditions such as lower soil moisture, and less spatial accessibility of microorganisms to
 530 fragmented litter as mentioned above, leading to a slower decomposition of root-litter in
 531 warmed than in ambient subsoil.

532 The faster and slower decomposition of hydrolysable lipids at warmed top- and subsoil,
 533 respectively, lead to depth-specific mean residence time (MRT) of molecular markers such as
 534 ω -hydroxy acids and diacids. In one previous study, hydrolysable lipids were revealed to have
 535 a decadal MRT of 32 to 34 years (Feng et al., 2010). At topsoil in warmed plots, only about
 536 40% of ω -hydroxy acids and diacids remained, whereas more (between 68% and 80% of these
 537 two markers) were left in subsoils (Supplementary *Table S2*), leading to a shorter MRT of these
 538 compound classes in the topsoil (3.4 years and 3.6 years, respectively) and longer in the subsoil



539 (between 6.3 and 15.0 years) (Supplementary *Table S3*). In ambient plots, the MRT of ω -
 540 hydroxy acids and diacids did not change much with depth (Supplementary *Table S3*), which
 541 has a similar trend as bulk root recovery in ambient plots. The molecular makers we analyzed
 542 had a shorter MRT, which could be related to the fact that they stem from grass roots (*Avena*
 543 *fatua*) with less lignin and lower C/N ratios than the mostly woody roots originating from the
 544 local vegetation at the site (Hicks Pries et al., 2018; Silver and Miya, 2001), and hydrolysable
 545 lipids without association to lignin could be steadily decomposed (Angst et al., 2016).
 546 However, an underestimation of MRT could exist in our study since we have a much shorter
 547 experimental duration compared to other studies (Feng et al., 2010).

548 Another striking finding is that there is accumulation of fatty acids in subsoil in ambient
 549 plots where the hydrolysable lipids were steadily decomposed (Fig. 4b). This accumulation of
 550 fatty acids is also observed in deep soil in DC ambient plots where root-litter was not added
 551 (Fig. 1b). The mass of fatty acids found in the soil after hydrolysis exceeds that in originally
 552 added labelled roots, implying another source for these additional fatty acids. The accumulation
 553 of this compound class is predominantly from an increase of octadecanoic acid ($C_{18:0}$ fatty
 554 acids), octadecenoic acid ($C_{18:1}$ fatty acids), and hexadecanoic acid ($C_{16:0}$ fatty acids)
 555 (Supplementary *Table S2*). It is noteworthy that there is no accumulation of fatty acids with a
 556 chain length larger than 20 (Supplementary *Fig. S1*), which is also confirmed by an on-average
 557 shorter carbon chain-length in DC ambient plots than in DC warmed plots Supplementary *Fig.*
 558 *S2*). Long-chain fatty acids are typically enriched in higher plant biomass, while the mid-length
 559 homologues are often enriched in microbial and plant biomass (Harwood and Russell, 1984).
 560 These additional fatty acids originate likely from microbial biomass, e.g. phospholipid fatty
 561 acids (PLFA) (Joergensen, 2022; Zelles, 1997), since these ester-linked microbial markers also
 562 contain fatty acids which could be released during hydrolyzation as non-bound free-extractable
 563 fatty acids were removed before hydrolysis. This is also confirmed by the presence of probably
 564 root-derived fatty acids, or other root-derived C has been metabolized by microorganisms and
 565 the ^{13}C signal is incorporated in microbial membrane lipids (Gunina et al., 2014).

566 Another possible reason for the accumulation of fatty acids could be preferential loss
 567 of certain other compound classes in hydrolysable lipids during their decomposition. Previous
 568 studies suggested contradictory theories of how suberin and cutin can depolymerize. One
 569 theory is simultaneous and similar decomposition of the compound classes (Riederer et al.,
 570 1993). Alternatively, long-chain (>16) ω -hydroxy and diacids could be more prone to be
 571 released (Naafs et al., 2005; Nierop et al., 2003), or monomers with only one functional group



such as *n*-alcohols could be preferentially decomposed due to their terminal position in polyesters (Mueller et al., 2013). Therefore, we cannot state whether fatty acids in our experiment were preferentially lost and taken up by microorganisms. However, the results of higher enrichment of ^{13}C signature in fatty acids in ambient plots support previous statements that microbial activity is higher in subsoil with ambient temperature than with warming, which is additionally validated by higher $\delta^{13}\text{C}$ values that are incorporated in PLFA (Pegoraro et al., submitted.).

Combining the results of root recovery in bulk soil and at molecular level we can notice that although the overall root-derived carbon recoveries are similar between warmed and ambient subsoil, a considerable amount of root-derived carbon is already incorporated in microbial biomass in ambient plots, meaning a slower decomposition of root-litter in warmed subsoil.

4.3 Minor priming effect of added ^{13}C -labelled root litter

Fresh biomass input can stimulate (prime) the decomposition of native, pre-existing SOM. This is especially relevant in subsoils, where SOM might have existed for a long time, from decades to millennia (Fontaine et al., 2007; Luo et al., 2019; Shahzad et al., 2018). Such priming could offset long-term carbon sequestration, especially in subsoil where there is usually substrate limitation (Bernard et al., 2022; Bingeman et al., 1953).

Three years after adding ^{13}C -labelled root tissues at three different soil depths, we found no evidence for significant priming across the whole soil profile, both for pre-existing bulk C and hydrolysable lipids. There could be several explanations. First, fresh carbon input was added only at the beginning of the incubation. Since priming is a temporary response to fresh carbon input (Schiedung et al., 2023) and is commonly strongest at the beginning of the incubation (Fontaine et al., 2007; Tao et al., 2024), this effect might become negligible after three years of incubation. Second, warming could suppress priming due to decreased N mining of microorganisms in native soil (Dong et al., 2024; Li et al., 2023; Sun et al., 2019). Blodgett Forest is limited in nitrogen and the added grass root-litter contains more nitrogen than the roots of native tree species (Hicks Pries et al., 2018; Silver and Miya, 2001). When native SOM is nitrogen deficient, and the added substrate contains nitrogen, as in our study, warming will stimulate the mineralization of the added substrate and release nitrogen from it for microbial growth (Feng and Zhu, 2021). Such a process could partially explain why we found negative priming (inhibition) for bulk subsoil SOM.



604 **4.4 Subsoil responds more heterogeneously than topsoil to warming**

605 One of the difficulties to implement an *in-situ* field warming experiment is the inherent
 606 heterogeneity and complexity of natural soil conditions, especially in subsoil.

607 Since the same amount of ^{13}C labelled root-litter was added at different depths, it could
 608 have different impacts on the microorganisms between top- and subsoil. Specifically, when the
 609 heterogeneous carbon concentrations between pairs of plots or even within the same plots were
 610 considered (Supplementary *Table S5*), the new input could contribute between 10% and 39%
 611 to the pre-existing carbon. This heterogeneity is partially reflected in ^{13}C -excess of bulk soil
 612 carbon (Fig. 2a), with larger error bars with depth. Although the root-litter was fully mixed
 613 with soil and the amount of added substrate is substantial for subsoil microorganisms, this does
 614 not mean that all the substrates could be accessed by microorganisms (Inagaki et al., 2023;
 615 Salomé et al., 2010), especially in warmed subsoil due to less abundant microorganisms
 616 compared to topsoil and their restricted mobility.

617 The different responses of root-litter decomposition between top- and subsoil with
 618 warming highlight the fundamental importance for regarding depth as a rudimentary factor for
 619 studying soil carbon dynamics. The large heterogeneity existing in subsoil spotlights the
 620 uncertainties in predicting subsoil's responses to climate change, especially when subsoil is
 621 considered for long-term carbon sequestration (Button et al., 2022; Sierra et al., 2024), and
 622 more focus should be drawn on observation into subsoil. To reduce the large heterogeneity in
 623 an experiment such as ours, a more realistic amount of root-litter added to individual depths
 624 could be achieved by first assessing root distribution across the whole soil profile via
 625 techniques such as minirhizotrons (Rahman et al., 2020), and then adjusting the added amount
 626 of root litter.

627 **5. Conclusions**

628 Natural ecosystems are complex and their response to warming is intricate, depending
 629 on many biotic and abiotic factors and their interactions. Warming accelerated the
 630 decomposition of root-derived carbon in topsoil after three years of incubation, but surprisingly
 631 not in the subsoil. This difference could be attributed to the fundamental differences of biotic
 632 and abiotic factors between top- and subsoil, which are further affected by environmental
 633 stress, such as warming.

634 Suberin markers, such as ω -hydroxy acids and diacids, are relatively more resistant
 635 compared to other root components, but they are less resistant to decomposition with warming



in topsoil. However, once the decomposition is slowed down in subsoil by warming due to unfavorable conditions such as lower microbial abundance and soil moisture, these molecular markers could be preserved in subsoil over one decade (Supplementary Table S3). Warming also altered the composition of hydrolysable lipids, especially in subsoil, with an accumulation of fatty acids. We interpreted the accumulation of fatty acids as potential evidence for the higher microbial activity and higher turnover rate of new OM in ambient than warming plots. It is noteworthy that the decomposition of added root-litter in natural subsoil with warming was heterogeneous, which obscured potentially existing trends with depth, and potential systematic differences between ambient and warmed plots.

Our experiment is one of the first *in-situ* long-term incubations on the effect of warming on the decomposition of simulated new substrates input at different soil depths in natural conditions at molecular level. The compound-specific isotope analysis leaves us a key message: Although after 3 years of incubation the recoveries of root-derived carbon are similar in subsoil regardless of temperature treatment, the carbon dynamics could be fundamentally changed by warming. The intrinsic chemical or thermodynamic properties may slow down the decomposition of chemically persistent molecules like hydrolysable lipids. However, in subsoil, the key factors influencing whether root-litter is transformed into long-term carbon storage are the decomposers' possibilities to access the substrates and their strategies to survive in harsh conditions with limited nutrients and substrates. The large natural heterogeneity of the investigated soil did not allow to identify a clear trend how subsoil responds to warming. Future *in-situ* observations should include both short-term (months) and long-term (several years to decade) observations to identify and quantify the time-resolved fate of new OM substrate and how the microbial community responds to warming.

Competing interests

The authors declare that they have no conflict of interest

Author contributions

EP shared resources and contributed to statistical analysis, writing review, and editing. MST applied for the funding, designed and maintained the warming experiment, contributed to statistical analysis, and writing review. CUZ conducted elemental analysis, introduced lipid analysis to me, and contributed to conceptualization, writing review and editing. GLBW supervised BS through the lipid analysis, contributed to methodology, conceptualization, data



669 interpretation and validation, writing review, and editing. MWIS applied for funding and
 670 conceived DEEP C project, contributed to conceptualization, data interpretation, writing
 671 review, and editing. BS conducted lipids analysis and data interpretation, contributed to writing
 672 original draft, statistical analysis, and editing.

673

674 **Acknowledgement**

675 We thank Nicholas Ofiti, Tatjana Speckert for introduction and help of lipid analysis
 676 methods, Thomas Keller, Barbara Siegfried and Yves Brügger for lab support.

677 This study was supported by the Swiss National Science Foundation (SNF) as the DEEP
 678 C project (200021_172744) and the Belowground Biogeochemistry Scientific Focus Area by
 679 the U.S. Department of Energy, Office of Science, Office of Biological and Environmental
 680 Research, Environmental System Science Program, under Contract Number DE-AC02-
 681 05CH11231.

682

683 **References**

684 Angst, G., Heinrich, L., Kögel-Knabner, I., and Mueller, C. W.: The fate of cutin and
 685 suberin of decaying leaves, needles and roots – Inferences from the initial decomposition of
 686 bound fatty acids, *Org. Geochem.*, 95, 81–92,
 687 <https://doi.org/10.1016/j.orggeochem.2016.02.006>, 2016.

688 Arndal, M. F., Tolver, A., Larsen, K. S., Beier, C., and Schmidt, I. K.: Fine root growth
 689 and vertical distribution in response to elevated CO₂, warming and drought in a mixed
 690 heathland–grassland, *Ecosystems*, 21, 15–30, <https://doi.org/10.1007/s10021-017-0131-2>,
 691 2018.

692 Bernard, L., Basile-Doelsch, I., Derrien, D., Fanin, N., Fontaine, S., Guenet, B., Karimi,
 693 B., Marsden, C., and Maron, P.-A.: Advancing the mechanistic understanding of the priming
 694 effect on soil organic matter mineralisation, *Funct. Ecol.*, 36, 1355–1377,
 695 <https://doi.org/10.1111/1365-2435.14038>, 2022.

696 Bhatti, A. A., Haq, S., and Bhat, R. A.: Actinomycetes benefaction role in soil and plant
 697 health, *Microb. Pathogenesis*, 111, 458–467, <https://doi.org/10.1016/j.micpath.2017.09.036>,
 698 2017.



- 699 Bingeman, C. W., Varner, J. E., and Martin, W. P.: The effect of the addition of organic
 700 materials on the decomposition of an organic soil, *Soil Sci. Soc. Am. J.*, 17, 34–38,
 701 <https://doi.org/10.2136/sssaj1953.03615995001700010008x>, 1953.
- 702 Button, E. S., Pett-Ridge, J., Murphy, D. V., Kuzyakov, Y., Chadwick, D. R., and Jones,
 703 D. L.: Deep-C storage: Biological, chemical and physical strategies to enhance carbon stocks
 704 in agricultural subsoils, *Soil Biol. Biochem.*, 170, 108697,
 705 <https://doi.org/10.1016/j.soilbio.2022.108697>, 2022.
- 706 Castanha, C., Zhu, B., Hicks Pries, C. E., Georgiou, K., and Torn, M. S.: The effects of
 707 heating, rhizosphere, and depth on root litter decomposition are mediated by soil moisture,
 708 *Biogeochemistry*, 137, 267–279, <https://doi.org/10.1007/s10533-017-0418-6>, 2018.
- 709 Chen, Y., Han, M., Yuan, X., Hou, Y., Qin, W., Zhou, H., Zhao, X., Klein, J. A., and
 710 Zhu, B.: Warming has a minor effect on surface soil organic carbon in alpine meadow
 711 ecosystems on the Qinghai–Tibetan Plateau, *Glob. Change Biol.*, 28, 1618–1629,
 712 <https://doi.org/10.1111/gcb.15984>, 2022.
- 713 DeAngelis, K. M., Pold, G., Topçuoğlu B. D., van Diepen, L. T. A., Varney, R. M.,
 714 Blanchard, J. L., Melillo, J., and Frey, S. D.: Long-term forest soil warming alters microbial
 715 communities in temperate forest soils, *Front. Microbiol.*, 6,
 716 <https://doi.org/10.3389/fmicb.2015.00104>, 2015.
- 717 Dijkstra, F. A., Zhu, B., and Cheng, W.: Root effects on soil organic carbon: a double-
 718 edged sword, *New Phytol.*, 230, 60–65, <https://doi.org/10.1111/nph.17082>, 2021.
- 719 Dong, H., Lin, J., Lu, J., Li, L., Yu, Z., Kumar, A., Zhang, Q., Liu, D., and Chen, B.:
 720 Priming effects of surface soil organic carbon decreased with warming: a global meta-analysis,
 721 *Plant Soil*, 500, 233–242, <https://doi.org/10.1007/s11104-022-05851-1>, 2024.
- 722 Dove, N. C., Torn, M. S., Hart, S. C., and Taş, N.: Metabolic capabilities mute positive
 723 response to direct and indirect impacts of warming throughout the soil profile, *Nat. Commun.*,
 724 12, 2089, <https://doi.org/10.1038/s41467-021-22408-5>, 2021.
- 725 Eckardt, N. A., Ainsworth, E. A., Bahuguna, R. N., Broadley, M. R., Busch, W.,
 726 Carpita, N. C., Castrillo, G., Chory, J., DeHaan, L. R., Duarte, C. M., Henry, A., Jagadish, S.
 727 V. K., Langdale, J. A., Leakey, A. D. B., Liao, J. C., Lu, K.-J., McCann, M. C., McKay, J. K.,
 728 Odeny, D. A., Jorge de Oliveira, E., Platten, J. D., Rabbi, I., Rim, E. Y., Ronald, P. C., Salt, D.
 729 E., Shigenaga, A. M., Wang, E., Wolfe, M., and Zhang, X.: Climate change challenges, plant
 730 science solutions, *Plant Cell*, 35, 24–66, <https://doi.org/10.1093/plcell/koac303>, 2023.



- 731 Eilers, K. G., Debenport, S., Anderson, S., and Fierer, N.: Digging deeper to find unique
 732 microbial communities: The strong effect of depth on the structure of bacterial and archaeal
 733 communities in soil, *Soil Biol. Biochem.*, 50, 58–65,
 734 <https://doi.org/10.1016/j.soilbio.2012.03.011>, 2012.
- 735 Epron, D., Bahn, M., Derrien, D., Lattanzi, F. A., Pumpanen, J., Gessler, A., Hogberg,
 736 P., Maillard, P., Dannoura, M., Gerant, D., and Buchmann, N.: Pulse-labelling trees to study
 737 carbon allocation dynamics: a review of methods, current knowledge and future prospects, *Tree*
 738 *Physiol*, 32, 776–798, <https://doi.org/10.1093/treephys/tps057>, 2012.
- 739 Fanin, N., Kardol, P., Farrell, M., Nilsson, M.-C., Gundale, M. J., and Wardle, D. A.:
 740 The ratio of Gram-positive to Gram-negative bacterial PLFA markers as an indicator of carbon
 741 availability in organic soils, *Soil Biol. Biochem.*, 128, 111–114,
 742 <https://doi.org/10.1016/j.soilbio.2018.10.010>, 2019.
- 743 Feng, J. and Zhu, B.: Global patterns and associated drivers of priming effect in
 744 response to nutrient addition, *Soil Biol. Biochem.*, 153, 108118,
 745 <https://doi.org/10.1016/j.soilbio.2020.108118>, 2021.
- 746 Feng, X., Xu, Y., Jaffé, R., Schlesinger, W. H., and Simpson, M. J.: Turnover rates of
 747 hydrolysable aliphatic lipids in Duke Forest soils determined by compound specific ^{13}C
 748 isotopic analysis, *Org. Geochem.*, 41, 573–579,
 749 <https://doi.org/10.1016/j.orggeochem.2010.02.013>, 2010.
- 750 Fierer, N., Schimel, J. P., and Holden, P. A.: Variations in microbial community
 751 composition through two soil depth profiles, *Soil Biol. Biochem.*, 35, 167–176,
 752 [https://doi.org/10.1016/S0038-0717\(02\)00251-1](https://doi.org/10.1016/S0038-0717(02)00251-1), 2003.
- 753 Fontaine, S., Barot, S., Barré, P., Bdioui, N., Mary, B., and Rumpel, C.: Stability of
 754 organic carbon in deep soil layers controlled by fresh carbon supply, *Nature*, 450, 277–280,
 755 <https://doi.org/10.1038/nature06275>, 2007.
- 756 van Gestel, N., Shi, Z., van Groenigen, K. J., Osenberg, C. W., Andresen, L. C., Dukes,
 757 J. S., Hovenden, M. J., Luo, Y., Michelsen, A., Pendall, E., Reich, P. B., Schuur, E. A. G., and
 758 Hungate, B. A.: Predicting soil carbon loss with warming, *Nature*, 554, E4–E5,
 759 <https://doi.org/10.1038/nature25745>, 2018.
- 760 Goodfellow, M. and Williams, S. T.: Ecology of actinomycetes, *Annu. Rev. Microbiol.*,
 761 37, 189–216, <https://doi.org/10.1146/annurev.mi.37.100183.001201>, 1983.
- 762 Graça, J.: Suberin: the biopolyester at the frontier of plants, *Front. Chem.*, 3,
 763 <https://doi.org/10.3389/fchem.2015.00062>, 2015.



- 764 Gunina, A., Dippold, M. A., Glaser, B., and Kuzyakov, Y.: Fate of low molecular
 765 weight organic substances in an arable soil: From microbial uptake to utilisation and
 766 stabilisation, *Soil Biol. Biochem.*, 77, 304–313, <https://doi.org/10.1016/j.soilbio.2014.06.029>,
 767 2014.
- 768 Harwood, J. L. and Russell, N. J.: *Lipids in Plants and Microbes*, Springer Netherlands,
 769 Dordrecht, 162 pp., <https://doi.org/10.1007/978-94-011-5989-0>, 1984.
- 770 Hicks Pries, C. E., Castanha, C., Porras, R. C., and Torn, M. S.: The whole-soil carbon
 771 flux in response to warming, *Science*, 355, 1420–1423,
 772 <https://doi.org/10.1126/science.aal1319>, 2017.
- 773 Hicks Pries, C. E., Sulman, B. N., West, C., O'Neill, C., Poppleton, E., Porras, R. C.,
 774 Castanha, C., Zhu, B., Wiedemeier, D. B., and Torn, M. S.: Root litter decomposition slows
 775 with soil depth, *Soil Biol. Biochem.*, 125, 103–114,
 776 <https://doi.org/10.1016/j.soilbio.2018.07.002>, 2018.
- 777 Huf, S., Krügener, S., Hirth, T., Rupp, S., and Zibek, S.: Biotechnological synthesis of
 778 long-chain dicarboxylic acids as building blocks for polymers, *Eur. J. Lipid Sci. Tech.*, 113,
 779 548–561, <https://doi.org/10.1002/ejlt.201000112>, 2011.
- 780 Inagaki, T. M., Possinger, A. R., Schweizer, S. A., Mueller, C. W., Hoeschen, C.,
 781 Zachman, M. J., Kourkoutis, L. F., Kögel-Knabner, I., and Lehmann, J.: Microscale spatial
 782 distribution and soil organic matter persistence in top and subsoil, *Soil Biol. Biochem.*, 178,
 783 108921, <https://doi.org/10.1016/j.soilbio.2022.108921>, 2023.
- 784 Jackson, R. B., Lajtha, K., Crow, S. E., Hugelius, G., Kramer, M. G., and Piñeiro, G.:
 785 The ecology of soil carbon: Pools, vulnerabilities, and biotic and abiotic controls, *Annu. Rev.*
 786 *Ecol. Evol. Syst.*, 48, 419–445, <https://doi.org/10.1146/annurev-ecolsys-112414-054234>,
 787 2017.
- 788 Jansen, B. and Wiesenberger, G. L. B.: Opportunities and limitations related to the
 789 application of plant-derived lipid molecular proxies in soil science, *SOIL*, 3, 211–234,
 790 <https://doi.org/10.5194/soil-3-211-2017>, 2017.
- 791 Joergensen, R. G.: Phospholipid fatty acids in soil—drawbacks and future prospects,
 792 *Biol. Fertil. Soils*, 58, 1–6, <https://doi.org/10.1007/s00374-021-01613-w>, 2022.
- 793 Keiluweit, M., Bougoure, J. J., Nico, P. S., Pett-Ridge, J., Weber, P. K., and Kleber,
 794 M.: Mineral protection of soil carbon counteracted by root exudates, *Nat. Clim. Change*, 5,
 795 588–595, <https://doi.org/10.1038/nclimate2580>, 2015.



- 796 Kim, K.-R. and Oh, D.-K.: Production of hydroxy fatty acids by microbial fatty acid-
 797 hydroxylation enzymes, *Biotechnol. Adv.*, 31, 1473–1485,
 798 <https://doi.org/10.1016/j.biotechadv.2013.07.004>, 2013.
- 799 Kim, S.-K. and Park, Y.-C.: Biosynthesis of ω -hydroxy fatty acids and related
 800 chemicals from natural fatty acids by recombinant *Escherichia coli*, *Appl. Microbiol.*
 801 *Biotechnol.*, 103, 191–199, <https://doi.org/10.1007/s00253-018-9503-6>, 2019.
- 802 Kolattukudy, P. E.: Biopolyester membranes of plants: Cutin and suberin, *Science*, 208,
 803 990–1000, <https://doi.org/10.1126/science.208.4447.990>, 1980.
- 804 Kuznetsova, A., Brockhoff, P. B., and Christensen, R. H. B.: lmerTest package: Tests
 805 in linear mixed effects models, *J. Stat. Softw.*, 82, 1–26, <https://doi.org/10.18637/jss.v082.i13>,
 806 2017.
- 807 Kwatcho Kengdo, S., Peršoh, D., Schindlbacher, A., Heinzle, J., Tian, Y., Wanek, W.,
 808 and Borken, W.: Long-term soil warming alters fine root dynamics and morphology, and their
 809 ectomycorrhizal fungal community in a temperate forest soil, *Glob. Change Biol.*, 00, 1–18,
 810 <https://doi.org/10.1111/gcb.16155>, 2022.
- 811 Li, X., Feng, J., Zhang, Q., and Zhu, B.: Warming inhibits the priming effect of soil
 812 organic carbon mineralization: A meta-analysis, *Sci. Total Environ.*, 904, 166170,
 813 <https://doi.org/10.1016/j.scitotenv.2023.166170>, 2023.
- 814 Luo, Z., Wang, G., and Wang, E.: Global subsoil organic carbon turnover times
 815 dominantly controlled by soil properties rather than climate, *Nat. Commun.*, 10, 3688,
 816 <https://doi.org/10.1038/s41467-019-11597-9>, 2019.
- 817 Lützow, M. v., Kögel-Knabner, I., Ekschmitt, K., Matzner, E., Guggenberger, G.,
 818 Marschner, B., and Flessa, H.: Stabilization of organic matter in temperate soils: mechanisms
 819 and their relevance under different soil conditions – a review, *Eur. J. Soil. Sci.*, 57, 426–445,
 820 <https://doi.org/10.1111/j.1365-2389.2006.00809.x>, 2006.
- 821 Malhotra, A., Brice, D. J., Childs, J., Graham, J. D., Hobbie, E. A., Stel, H. V., Feron,
 822 S. C., Hanson, P. J., and Iversen, C. M.: Peatland warming strongly increases fine-root growth,
 823 *PNAS*, 117, 17627–17634, <https://doi.org/10.1073/pnas.2003361117>, 2020.
- 824 Meier, I. C. and Leuschner, C.: Belowground drought response of European beech: fine
 825 root biomass and carbon partitioning in 14 mature stands across a precipitation gradient, *Glob.*
 826 *Change Biol.*, 14, 2081–2095, <https://doi.org/10.1111/j.1365-2486.2008.01634.x>, 2008.
- 827 Melillo, J. M., Frey, S. D., DeAngelis, K. M., Werner, W. J., Bernard, M. J., Bowles,
 828 F. P., Pold, G., Knorr, M. A., and Grandy, A. S.: Long-term pattern and magnitude of soil



- 829 carbon feedback to the climate system in a warming world, *Science*, 358, 101–105,
 830 <https://doi.org/10.1126/science.aan2874>, 2017.
- 831 Metze, D., Schneckner, J., De Carlan, C. L. N., Bhattarai, B., Verbruggen, E., Ostonen,
 832 I., Janssens, I. A., Sigurdsson, B. D., Hausmann, B., Kaiser, C., and Richter, A.: Soil warming
 833 increases the number of growing bacterial taxa but not their growth rates, *Sci. Adv.*, 10,
 834 eadk6295, <https://doi.org/10.1126/sciadv.adk6295>, 2024.
- 835 Mohan, T. and El-Halwagi, M. M.: An algebraic targeting approach for effective
 836 utilization of biomass in combined heat and power systems through process integration, *Clean*
 837 *Technol. Environ.*, 9, 13–25, <https://doi.org/10.1007/s10098-006-0051-x>, 2007.
- 838 Mueller, K. E., Polissar, P. J., Oleksyn, J., and Freeman, K. H.: Differentiating
 839 temperate tree species and their organs using lipid biomarkers in leaves, roots and soil, *Org.*
 840 *Geochem.*, 52, 130–141, <https://doi.org/10.1016/j.orggeochem.2012.08.014>, 2012.
- 841 Mueller, K. E., Eissenstat, D. M., Müller, C. W., Oleksyn, J., Reich, P. B., and Freeman,
 842 K. H.: What controls the concentration of various aliphatic lipids in soil?, *Soil Biol. Biochem.*,
 843 63, 14–17, <https://doi.org/10.1016/j.soilbio.2013.03.021>, 2013.
- 844 Naafs, D. F. W., Nierop, K. G. J., Van Bergen, P. F., and De Leeuw, J. W.: Changes in
 845 the molecular composition of ester-bound aliphatics with depth in an acid andic forest soil,
 846 *Geoderma*, 127, 130–136, <https://doi.org/10.1016/j.geoderma.2004.11.022>, 2005.
- 847 Naylor, D., McClure, R., and Jansson, J.: Trends in microbial community composition
 848 and function by soil depth, *Microorganisms*, 10, 540,
 849 <https://doi.org/10.3390/microorganisms10030540>, 2022.
- 850 Nierop, K. G. J., Naafs, D. F. W., and Verstraten, J. M.: Occurrence and distribution of
 851 ester-bound lipids in Dutch coastal dune soils along a pH gradient, *Org. Geochem.*, 34, 719–
 852 729, [https://doi.org/10.1016/S0146-6380\(03\)00042-1](https://doi.org/10.1016/S0146-6380(03)00042-1), 2003.
- 853 Ofiti, N. O. E., Zosso, C. U., Soong, J. L., Solly, E. F., Torn, M. S., Wiesenberg, G. L.
 854 B., and Schmidt, M. W. I.: Warming promotes loss of subsoil carbon through accelerated
 855 degradation of plant-derived organic matter, *Soil Biol. Biochem.*, 156, 108185,
 856 <https://doi.org/10.1016/j.soilbio.2021.108185>, 2021.
- 857 Ofiti, N. O. E., Schmidt, M. W. I., Abiven, S., Hanson, P. J., Iversen, C. M., Wilson, R.
 858 M., Kostka, J. E., Wiesenberg, G. L. B., and Malhotra, A.: Climate warming and elevated CO₂
 859 alter peatland soil carbon sources and stability, *Nat. Commun.*, 14, 7533,
 860 <https://doi.org/10.1038/s41467-023-43410-z>, 2023.



- 861 Olson, J. S.: Energy storage and the balance of producers and decomposers in
862 ecological systems, *Ecology*, 44, 322–331, <https://doi.org/10.2307/1932179>, 1963.
- 863 Parts, K., Tedersoo, L., Schindlbacher, A., Sigurdsson, B. D., Leblans, N. I. W.,
864 Oddsdóttir, E. S., Borken, W., and Ostonen, I.: Acclimation of fine root systems to soil
865 warming: Comparison of an experimental setup and a natural soil temperature gradient,
866 *Ecosystems*, 22, 457–472, <https://doi.org/10.1007/s10021-018-0280-y>, 2019.
- 867 Pegoraro, E., Zosso, C. U., Wiesenberger, G. L. B., Castanha, C., Hicks Pries, C., Porras,
868 R., Soong, J. L., Schmidt, M. W. I., and Torn, M. S.: Depth-dependent microbial response to
869 simulated increased root growth, submitted.
- 870 Poirier, V., Roumet, C., and Munson, A. D.: The root of the matter: Linking root traits
871 and soil organic matter stabilization processes, *Soil Biol. Biochem.*, 120, 246–259,
872 <https://doi.org/10.1016/j.soilbio.2018.02.016>, 2018.
- 873 Pold, G., Billings, A. F., Blanchard, J. L., Burkhardt, D. B., Frey, S. D., Melillo, J. M.,
874 Schnabel, J., van Diepen, L. T. A., and DeAngelis, K. M.: Long-term warming alters
875 carbohydrate degradation potential in temperate forest soils, *Appl. Environ. Microbiol.*, 82,
876 6518–6530, <https://doi.org/10.1128/AEM.02012-16>, 2016.
- 877 R Core Team (2024). *_R: A language and environment for statistical computing_*. R
878 Foundation for Statistical Computing, Vienna, Austria, available at: [https://www.R-](https://www.R-project.org/)
879 [project.org/](https://www.R-project.org/) (last access: 13 January 2025), 2024
- 880 Rahman, G., Sohag, H., Chowdhury, R., Wahid, K. A., Dinh, A., Arcand, M., and Vail,
881 S.: SoilCam: A fully automated Minirhizotron using Multispectral Imaging for root activity
882 monitoring, *Sensors*, 20, 787, <https://doi.org/10.3390/s20030787>, 2020.
- 883 Rasse, D. P., Rumpel, C., and Dignac, M.-F.: Is soil carbon mostly root carbon?
884 Mechanisms for a specific stabilisation, *Plant Soil*, 269, 341–356,
885 <https://doi.org/10.1007/s11104-004-0907-y>, 2005.
- 886 Riederer, M., Matzke, K., Ziegler, F., and Kögel-Knabner, I.: Occurrence, distribution
887 and fate of the lipid plant biopolymers cutin and suberin in temperate forest soils, *Org.*
888 *Geochem.*, 20, 1063–1076, [https://doi.org/10.1016/0146-6380\(93\)90114-Q](https://doi.org/10.1016/0146-6380(93)90114-Q), 1993.
- 889 Rumpel, C. and Kögel-Knabner, I.: Deep soil organic matter—a key but poorly
890 understood component of terrestrial C cycle, *Plant Soil*, 338, 143–158,
891 <https://doi.org/10.1007/s11104-010-0391-5>, 2011.
- 892 Rumpel, C., Chabbi, A., and Marschner, B.: Carbon Storage and Sequestration in
893 Subsoil Horizons: Knowledge, Gaps and Potentials, in: *Recarbonization of the Biosphere:*



- 894 Ecosystems and the Global Carbon Cycle, edited by: Lal, R., Lorenz, K., Hüttl, R. F.,
 895 Schneider, B. U., and von Braun, J., Springer Netherlands, Dordrecht, 445–464,
 896 https://doi.org/10.1007/978-94-007-4159-1_20, 2012.
- 897 Salomé, C., Nunan, N., Pouteau, V., Lerch, T. Z., and Chenu, C.: Carbon dynamics in
 898 topsoil and in subsoil may be controlled by different regulatory mechanisms, *Glob. Change*
 899 *Biol.*, 16, 416–426, <https://doi.org/10.1111/j.1365-2486.2009.01884.x>, 2010.
- 900 Scharlemann, J. P., Tanner, E. V., Hiederer, R., and Kapos, V.: Global soil carbon:
 901 understanding and managing the largest terrestrial carbon pool, *Carbon Manag.*, 5, 81–91,
 902 <https://doi.org/10.4155/cmt.13.77>, 2014.
- 903 Schenk, H. J. and Jackson, R. B.: Mapping the global distribution of deep roots in
 904 relation to climate and soil characteristics, *Geoderma*, 126, 129–140,
 905 <https://doi.org/10.1016/j.geoderma.2004.11.018>, 2005.
- 906 Schiedung, M., Don, A., Beare, M. H., and Abiven, S.: Soil carbon losses due to
 907 priming moderated by adaptation and legacy effects, *Nat. Geosci.*, 16, 909–914,
 908 <https://doi.org/10.1038/s41561-023-01275-3>, 2023.
- 909 Shahzad, T., Rashid, M. I., Maire, V., Barot, S., Perveen, N., Alvarez, G., Mougin, C.,
 910 and Fontaine, S.: Root penetration in deep soil layers stimulates mineralization of millennia-
 911 old organic carbon, *Soil Biol. Biochem.*, 124, 150–160,
 912 <https://doi.org/10.1016/j.soilbio.2018.06.010>, 2018.
- 913 Sierra, C. A., Ahrens, B., Bolinder, M. A., Braakhekke, M. C., von Fromm, S., Kätterer,
 914 T., Luo, Z., Parvin, N., and Wang, G.: Carbon sequestration in the subsoil and the time required
 915 to stabilize carbon for climate change mitigation, *Glob. Change Biol.*, 30, e17153,
 916 <https://doi.org/10.1111/gcb.17153>, 2024.
- 917 Silver, W. L. and Miya, R. K.: Global patterns in root decomposition: comparisons of
 918 climate and litter quality effects, *Oecologia*, 129, 407–419,
 919 <https://doi.org/10.1007/s004420100740>, 2001.
- 920 Sokol, N. W. and Bradford, M. A.: Microbial formation of stable soil carbon is more
 921 efficient from belowground than aboveground input, *Nat. Geosci.*, 12, 46–53,
 922 <https://doi.org/10.1038/s41561-018-0258-6>, 2019.
- 923 Soong, J. L., Phillips, C. L., Ledna, C., Koven, C. D., and Torn, M. S.: CMIP5 models
 924 predict rapid and deep soil warming over the 21st century, *J. Geophys. Res. Biogeosci.*, 125,
 925 <https://doi.org/10.1029/2019JG005266>, 2020.



- 926 Soong, J. L., Castanha, C., Hicks Pries, C. E., Ofiti, N., Porras, R. C., Riley, W. J.,
 927 Schmidt, M. W. I., and Torn, M. S.: Five years of whole-soil warming led to loss of subsoil
 928 carbon stocks and increased CO₂ efflux, *Sci. Adv.*, 7, eabd1343,
 929 <https://doi.org/10.1126/sciadv.abd1343>, 2021.
- 930 Speckert, T. C., Petibon, F., and Wiesenberger, G. L. B.: Late-season biosynthesis of leaf
 931 fatty acids and n-alkanes of a mature beech (*Fagus sylvatica*) tree traced via ¹³CO₂ pulse-chase
 932 labelling and compound-specific isotope analysis, *Front. Plant Sci.*, 13, 1029026,
 933 <https://doi.org/10.3389/fpls.2022.1029026>, 2023.
- 934 Spohn, M., Klaus, K., Wanek, W., and Richter, A.: Microbial carbon use efficiency and
 935 biomass turnover times depending on soil depth – Implications for carbon cycling, *Soil Biol.*
 936 *Biochem.*, 96, 74–81, <https://doi.org/10.1016/j.soilbio.2016.01.016>, 2016.
- 937 IPCC: Climate Change 2013: The Physical Science Basis. Contribution of Working
 938 Group I to the Fifth Assessment Report of the Intergovernmental Panel on Climate Change,
 939 edited by: Stocker, T. F., Qin, D., Plattner, G.-K., Tignor, M., Allen, S. K., Boschung, J., Nauels,
 940 A., Xia, Y., Bex, V., and Midgley, P. M., Cambridge University Press, Cambridge, UK and
 941 New York, NY, USA, 2013.
- 942 Sun, Z., Liu, S., Zhang, T., Zhao, X., Chen, S., and Wang, Q.: Priming of soil organic
 943 carbon decomposition induced by exogenous organic carbon input: a meta-analysis, *Plant Soil*,
 944 443, 463–471, <https://doi.org/10.1007/s11104-019-04240-5>, 2019.
- 945 Tao, X., Yang, Z., Feng, J., Jian, S., Yang, Y., Bates, C. T., Wang, G., Guo, X., Ning,
 946 D., Kempher, M. L., Liu, X. J. A., Ouyang, Y., Han, S., Wu, L., Zeng, Y., Kuang, J., Zhang,
 947 Y., Zhou, X., Shi, Z., Qin, W., Wang, J., Firestone, M. K., Tiedje, J. M., and Zhou, J.:
 948 Experimental warming accelerates positive soil priming in a temperate grassland ecosystem,
 949 *Nat. Commun.*, 15, 1178, <https://doi.org/10.1038/s41467-024-45277-0>, 2024.
- 950 Védère, C., Vieublé Gonod, L., Pouteau, V., Girardin, C., and Chenu, C.: Spatial and
 951 temporal evolution of detritusphere hotspots at different soil moistures, *Soil Biol. Biochem.*,
 952 150, 107975, <https://doi.org/10.1016/j.soilbio.2020.107975>, 2020.
- 953 Védère, C., Lebrun, M., Honvault, N., Aubertin, M.-L., Girardin, C., Garnier, P.,
 954 Dignac, M.-F., Houben, D., and Rumpel, C.: How does soil water status influence the fate of
 955 soil organic matter? A review of processes across scales, *Earth-Sci. Rev.*, 234, 104214,
 956 <https://doi.org/10.1016/j.earscirev.2022.104214>, 2022.
- 957 Verbrigghe, N., Leblans, N. I. W., Sigurdsson, B. D., Vicca, S., Fang, C., Fuchslueger,
 958 L., Soong, J. L., Weedon, J. T., Poeplau, C., Ariza-Carricondo, C., Bahn, M., Guenet, B.,



- 959 Gundersen, P., Gunnarsdóttir, G. E. G., Kätterer, T., Liu, Z., Maljanen, M., Maraño-Jiménez,
960 S., Meeran, K., Oddsdóttir, E. S., Ostonen, I., Peñuelas, J., Richter, A., Sardans, J., Sigurðsson,
961 P., Torn, M. S., Van Bodegom, P. M., Verbruggen, E., Walker, T. W. N., Wallander, H., and
962 Janssens, I. A.: Soil carbon loss in warmed subarctic grasslands is rapid and restricted to
963 topsoil, *Biogeosciences*, 19, 3381–3393, <https://doi.org/10.5194/bg-2021-338>, 2022.
- 964 Walker, T. W. N., Kaiser, C., Strasser, F., Herbold, C. W., Leblans, N. I. W., Woebken,
965 D., Janssens, I. A., Sigurdsson, B. D., and Richter, A.: Microbial temperature sensitivity and
966 biomass change explain soil carbon loss with warming, *Nat. Clim. Change*, 8, 885–889,
967 <https://doi.org/10.1038/s41558-018-0259-x>, 2018.
- 968 Wang, J., Defrenne, C., McCormack, M. L., Yang, L., Tian, D., Luo, Y., Hou, E., Yan,
969 T., Li, Z., Bu, W., Chen, Y., and Niu, S.: Fine-root functional trait responses to experimental
970 warming: a global meta-analysis, *New Phytol.*, 230, 1856–1867,
971 <https://doi.org/10.1111/nph.17279>, 2021.
- 972 Wang, P., Limpens, J., Mommer, L., van Ruijven, J., Nauta, A. L., Berendse, F.,
973 Schaepman-Strub, G., Blok, D., Maximov, T. C., and Heijmans, M. M. P. D.: Above- and
974 below-ground responses of four tundra plant functional types to deep soil heating and surface
975 soil fertilization, *J. Ecol.*, 105, 947–957, <https://doi.org/10.1111/1365-2745.12718>, 2017.
- 976 Wiesenberg, G. L. B. and Gocke, M. I.: Analysis of Lipids and Polycyclic Aromatic
977 Hydrocarbons as Indicators of Past and Present (Micro)Biological Activity, in: *Hydrocarbon
978 and Lipid Microbiology Protocols*, edited by: McGenity, T. J., Timmis, K. N., and Nogales,
979 B., Springer Berlin Heidelberg, Berlin, Heidelberg, 61–91,
980 https://doi.org/10.1007/8623_2015_157, 2017.
- 981 Wiesenberg, G. L. B., Schwarzbauer, J., Schmidt, M. W. I., and Schwark, L.: Plant and
982 soil lipid modification under elevated atmospheric CO₂ conditions: II. Stable carbon isotopic
983 values ($\delta^{13}\text{C}$) and turnover, *Org. Geochem.*, 39, 103–117,
984 <https://doi.org/10.1016/j.orggeochem.2007.09.006>, 2008.
- 985 Xu, T., Chen, X., Hou, Y., and Zhu, B.: Changes in microbial biomass, community
986 composition and diversity, and functioning with soil depth in two alpine ecosystems on the
987 Tibetan plateau, *Plant Soil*, 459, 137–153, <https://doi.org/10.1007/s11104-020-04712-z>, 2021.
- 988 Yaffar, D., Wood, T. E., Reed, S. C., Branoff, B. L., Cavaleri, M. A., and Norby, R. J.:
989 Experimental warming and its legacy effects on root dynamics following two hurricane
990 disturbances in a wet tropical forest, *Glob. Change Biol.*, 27, 6423–6435,
991 <https://doi.org/10.1111/gcb.15870>, 2021.



992 Zelles, L.: Phospholipid fatty acid profiles in selected members of soil microbial
 993 communities, *Chemosphere*, 35, 275–294, [https://doi.org/10.1016/S0045-6535\(97\)00155-0](https://doi.org/10.1016/S0045-6535(97)00155-0),
 994 1997.
 995 Zhang, W., Hu, W., Zhu, Q., Niu, M., An, N., Feng, Y., Kawamura, K., and Fu, P.:
 996 Hydroxy fatty acids in the surface Earth system, *Sci. Total Environ.*, 906, 167358,
 997 <https://doi.org/10.1016/j.scitotenv.2023.167358>, 2024.
 998 Zosso, C. U., Ofiti, N. O. E., Soong, J. L., Solly, E. F., Torn, M. S., Huguet, A.,
 999 Wiesenberg, G. L. B., and Schmidt, M. W. I.: Whole-soil warming decreases abundance and
 1000 modifies the community structure of microorganisms in the subsoil but not in surface soil,
 1001 *SOIL*, 7, 477–494, <https://doi.org/10.5194/soil-7-477-2021>, 2021.
 1002 Zosso, C. U., Ofiti, N. O. E., Torn, M. S., Wiesenberg, G. L. B., and Schmidt, M. W.
 1003 I.: Rapid loss of complex polymers and pyrogenic carbon in subsoils under whole-soil
 1004 warming, *Nat. Geosci.*, 16, 344–348, <https://doi.org/10.1038/s41561-023-01142-1>, 2023.
 1005